

# Equation-of-Motion Coupled-Cluster Methods for Open-Shell and Electronically Excited Species: The Hitchhiker's Guide to Fock Space

Anna I. Krylov

Department of Chemistry, University of Southern California, Los Angeles, California  
90089-0482; email: krylov@usc.edu

Annu. Rev. Phys. Chem. 2008. 59:433–62

First published online as a Review in Advance on  
January 3, 2008

The *Annual Review of Physical Chemistry* is online at  
<http://physchem.annualreviews.org>

This article's doi:  
10.1146/annurev.physchem.59.032607.093602

Copyright © 2008 by Annual Reviews.  
All rights reserved

0066-426X/08/0505-0433\$20.00

## Key Words

electronic structure, diradicals, triradicals, spin-flip

## Abstract

The equation-of-motion coupled-cluster (EOM-CC) approach is a versatile electronic-structure tool that allows one to describe a variety of multiconfigurational wave functions within single-reference formalism. This review provides a guide to established EOM methods illustrated by examples that demonstrate the types of target states currently accessible by EOM. It focuses on applications of EOM-CC to electronically excited and open-shell species. The examples emphasize EOM's advantages for selected situations often perceived as multireference cases [e.g., interacting states of different nature, Jahn-Teller (JT) and pseudo-JT states, dense manifolds of ionized states, diradicals, and triradicals]. I also discuss limitations and caveats and offer practical solutions to some problematic situations. The review also touches on some formal aspects of the theory and important current developments.

---

**MR:** multireference  
**CI:** configuration interaction  
**CC:** coupled cluster  
**EOM:** equation of motion  
**JT:** Jahn-Teller

---

## 1. INTRODUCTION

The Infinite Improbability Drive is a wonderful new method of crossing vast interstellar distances in a mere nothingth of a second, without all that tedious mucking about in hyperspace.

*The Hitchhiker's Guide to the Galaxy*, Douglas Adams

When a covalent bond breaks, a pair of radicals is formed. That is why the mechanisms of many chemical reactions involve open-shell species as transient intermediates or transition states. Photosynthesis and vision, the interaction of anticancer drugs with tumor cells, enzyme catalysis, combustion, and the atmospheric ozone production/decomposition cycles are just a few examples. Unraveling the mechanisms of such reactions requires understanding the electronic structure of open-shell species and, therefore, relies heavily on *ab initio* calculations.

Despite their important role in chemistry, the theoretical modeling of open-shell and electronically excited (EE) species remains a major challenge because of electronic (near) degeneracies, which are prevalent in open-shell species. Orbital degeneracy results in multiconfigurational wave functions and closely lying interacting electronic states. Thus, the well-developed hierarchy of ground-state methods (1, 2) based on the assumption that the wave function is dominated by a single Slater determinant breaks down, as the Hartree-Fock method fails to provide a qualitatively correct zero-order description.

Traditionally, these chemically important situations were treated by multireference (MR) methods (3), which are generally formulated in Hilbert space and always begin by constructing an appropriate zero-order wave function including all the important (as deemed by the user) configurations. This is usually achieved using the multiconfigurational self-consistent-field method (4, 5). These wave functions are constructed and optimized for each state of interest and are subsequently improved by including dynamical correlation through perturbation theory, configuration interaction (CI), or coupled-cluster (CC) formalisms.

Equation-of-motion (EOM) methods (6–14) employ a radically different approach exploiting Fock space. Instead of, as one might say, mucking about in the Hilbert space, they describe the entire manifold of multiconfigurational target states within a single-reference formalism. This requires finding a path in Fock space that connects the reference state and the target state through the general excitation operators. This review provides a guide to established EOM methods illustrated by examples demonstrating the types of target states currently accessible by EOM (see Sections 2 and 3). The examples emphasize EOM's advantages for selected situations [e.g., interacting states of different natures, Jahn-Teller (JT) and pseudo-JT states, dense manifolds of ionized states, diradicals, and triradicals]. Section 4 presents a more rigorous formal discussion, which may be skipped by those not inclined to dwell on the meaning of equations. Finally, Sections 5 and 6 discuss the limitations of existing EOM methods, as well as important developments.

This article by no means provides a comprehensive overview of the history of EOM-CC methodology or the current state of the field. I refer interested readers to several more detailed reviews (15–20). Moreover, I do not discuss EOM-CC's

relationship to the closely related linear-response CC formalism (21–24), or symmetry-adapted cluster CI methods (25, 26), as well as propagator approaches exploring similar ideas. Genuinely MR-CC methods (15, 17, 27–29) are also outside the scope of the review.

---

**CCSD:** coupled cluster with single and double substitutions

---

## 2. EOM IN A NUTSHELL: “DON’T PANIC!”

Conceptually, EOM is similar to CI: One finds the target EOM states by diagonalizing the so-called similarity transformed Hamiltonian  $\tilde{H} \equiv e^{-T} H e^T$ :

$$\tilde{H}R = ER, \quad (1)$$

$$L\tilde{H} = EL, \quad (2)$$

$$L_I R_J = \delta_{IJ}, \quad (3)$$

where  $T$ ,  $R$ , and  $L^+$  are general excitation operators with respect to the reference  $|\Phi_0\rangle$ . This review is concerned strictly with the single-reference formulation of EOM, that is, when the reference  $|\Phi_0\rangle$  is a single Slater determinant. The choice of  $|\Phi_0\rangle$  defines the Hartree-Fock vacuum (i.e., the separation of the orbital space into occupied and virtual subspaces), and  $T$ ,  $R$ , and  $L^+$  are excitation operators with respect to this vacuum. We adhere to the following convention: Indexes  $i, j, \dots$  are reserved for the orbitals occupied in the reference determinant  $|\Phi_0\rangle$ ; indexes  $a, b, \dots$  are used for unoccupied orbitals; and  $p, q, \dots$  are used in the general case (i.e., when an orbital can be either occupied or virtual).

Regardless of the choice of  $T$ , the spectrum of  $\tilde{H}$  is exactly the same as that of the original Hamiltonian  $H$ —thus, in the limit of the complete many-electron basis set, EOM is identical to full CI. Because  $\tilde{H}$  is no longer Hermitian, its left and right eigenstates are not Hermitian conjugates (rather, they can be chosen to form a biorthogonal set) even when  $\tilde{H}$  is diagonalized in the complete basis yielding the exact energies and states. One can obtain eigenstates  $\Psi$  of the bare Hamiltonian  $H$  from the eigenstates of  $\tilde{H}$  as follows:

$$|\Psi\rangle = e^T R |\Phi_0\rangle = R e^T |\Phi_0\rangle. \quad (4)$$

In a more practical case of a truncated basis (e.g., when  $T$  and  $R$  are truncated at single and double excitations), the EOM models are numerically superior to the corresponding CI models (30) because correlation effects are folded in the transformed Hamiltonian. Moreover, the truncated EOM models are rigorously size consistent (or, more precisely, size intensive; see Section 3.1.3) (23, 31–34), provided that the amplitudes  $T$  satisfy the CC equations (35, 36) for the reference state  $|\Phi_0\rangle$  and are truncated at a sufficiently high level of excitation, consistent with that of  $R$ :

$$\langle \Phi_\mu | \tilde{H} | \Phi_0 \rangle = 0, \quad (5)$$

where  $\Phi_\mu$  denotes  $\mu$ -tuply excited determinants [e.g.,  $\{\Phi_i^a, \Phi_{ij}^{ab}\}$  in the case of coupled cluster with single and double substitutions (CCSD)].

Once the occupied and virtual subspaces are defined, EOM is invariant with respect to unitary transformations of the occupied or virtual orbitals, unless active-space models are employed. This invariance and partial transferability of the reference-state

relaxation described by  $\exp(T_1)$  explain why target states of different character are well described by EOM-CCSD using the same set of (uncorrelated) orbitals without explicit orbital optimization,  $R_2$  taking care of the differential orbital-relaxation effects.

Usually (9, 37) but not necessarily (38, 39), the cluster operator  $T$  is truncated at the same level as the EOM operators  $R$  and  $L^+$ . When this is the case, or when  $T$  is truncated at a higher excitation level than  $R$ , the reference determinant  $|\Phi_0\rangle$  is an eigenstate of  $\tilde{H}$  in the subspace of up to  $n$ -tuple excited determinants, the corresponding eigenvalue being  $E_0 = \langle \Phi_0 | \tilde{H} | \Phi_0 \rangle$ .

The computational scalings of EOM-CC and CI methods are identical (e.g., both EOM-CCSD and CI with single and double substitutions scale as  $N^6$ ). By combining different types of excitation operators and references  $|\Phi_0\rangle$ , one can access different groups of target states as explained below. For example, EE states can be described when the reference  $|\Phi_0\rangle$  corresponds to the ground-state wave function, and the operators  $R$  conserve the number of electrons and a total spin (9, 22, 23). In the ionized/electron attached EOM models (11–14, 40, 41), the operators  $R$  are not electron conserving (i.e., they include a different number of creation and annihilation operators)—these models can accurately treat ground and excited states of doublet radicals, charge-transfer, and other open-shell systems. Finally, the EOM spin-flip (SF) method (10, 42), in which the excitation operators include SF, allows one to access diradicals, triradicals, and bond breaking without using spin- and symmetry-broken unrestricted Hartree-Fock references or MR treatment.

### 3. HOW TO HITCH A RIDE IN FOCK SPACE: THE CHOICE OF REFERENCE AND EXCITATION OPERATOR

Here is what to do if you want to get a lift from a Vagon: forget it.

*The Hitchhiker's Guide to the Galaxy*, Douglas Adams

The crux of setting up a successful EOM calculation is finding a shortcut in Fock space, that is, identifying a well-behaved reference state  $\Phi_0$  from which the target states can be accessed by a general excitation operator, preferably, of low excitation level. The excitation operator thus connects the initial and target sectors of the Fock space. Below we describe several choices of references and excitation operators and illustrate the capabilities of the resulting EOM models.

#### 3.1. EOM for Electronically Excited States: EOM-EE

Describing EE states is, perhaps, the most obvious (and conceptually similar to CI) application of EOM. In this case, the EOM operators are of  $hp$ ,  $2h2p$ ,  $\dots$  type (where  $hp$  stands for the hole-particle) and conserve the number of  $\alpha$  and  $\beta$  electrons:

$$R^{EE} = \sum_{ia} r_i^a a^+ i + \frac{1}{4} \sum_{ijab} r_{ij}^{ab} a^+ b^+ j i + \dots, \quad (6)$$

where only  $M_s = 0$  strings of creation and annihilation operators are retained, yielding, for example,  $\alpha \rightarrow \alpha$  and  $\beta \rightarrow \beta$  excitations. Moreover, in the case of restricted

references, one can trivially spin adapt the operators  $R$  to form either singlet or triplet excitations:

$$\begin{aligned} R^s &= \sum_{ia} r_i^a (a_\alpha^+ i_\alpha + a_\beta^+ i_\beta) + \dots, \\ R^t &= \sum_{ia} r_i^a (a_\alpha^+ i_\alpha - a_\beta^+ i_\beta) + \dots \end{aligned} \quad (7)$$

---

MO: molecular orbital

---

When applied to a closed-shell reference,  $R^s$  and  $R^t$  generate properly spin-adapted singlet and  $M_s = 0$  triplet states, respectively; however, in the case of open-shell references (e.g., doublets), the resulting states are not spin adapted (18).

The CI-like form of the EOM-EE excitation operator enables access to multi-configurational open-shell wave functions, exactly and nearly degenerate states (e.g., JT pairs), as well as interacting states of different character (i.e., Rydberg and valence states). The examples below illustrate some of these features. The conservative estimate of EOM-EE-CCSD error bars for excitation energies is 0.1–0.3-eV accuracy (43), whereas relative spacing of the excited states is usually reproduced more accurately.

**3.1.1. EOM for excited states of mixed character: Rydberg-valence interactions in diazomethane.** **Figure 1** shows relevant molecular orbitals (MOs) and electronic configurations of several excited states of diazomethane (44). The states are derived by excitations from the highest occupied molecular orbital (HOMO), which is of bonding  $\pi_{CN}$  character, to the corresponding  $\pi^*$  and the three  $3p$  Rydberg-type orbitals. Note that the open-shell character of the singlet excited states is easily described by the EOM-EE ansatz. Moreover, pairs of open-shell determinants appear with equal weights (see Equation 7), thus ensuring proper spin symmetry. This naturally follows from the EOM eigenproblem, without enforcing Equation 7 on the EOM amplitudes.

Whereas the  $2^1A_2$  and  $2^1B_1$  states are predominantly Rydberg, as found from the EOM amplitudes and spatial extents of their wave functions, the two  $A_1$  states are of a mixed Rydberg-valence character. The lower state is predominantly valence, whereas the upper one is dominated by  $\pi \rightarrow 3p_x$  excitation. This strong interaction between the two states, which are more than 1 eV apart, has important consequences. For example, the  $3^1A_1$  ( $3p_x$ ) state borrows intensity from the valence state. Moreover, its equilibrium geometry and frequencies strongly deviate from those of the cation (and the other two Rydberg states), contrary to considerations based on the character of the  $3p_x$  orbital (see **Figure 1**), which is perpendicular to the molecular plane and, therefore, should be the least perturbed by the cation core.

Despite the mixed character of the interacting states (which would ordinarily be thought of as representing an MR situation), their wave functions are of singly excited character; that is, all the leading configurations appear at single excitations from the reference  $\Phi_0$ . Thus, EOM-CC describes these states with the same accuracy as pure Rydberg or valence states and is capable of correctly reproducing the degree of the mixing, provided, of course, an appropriate one-electron basis set is employed. Reproducing this type of interaction within MR formalism would require careful crafting of the active space at the multiconfigurational self-consistent-field level and subsequent inclusion of dynamical correlation. The popular B3LYP variant of

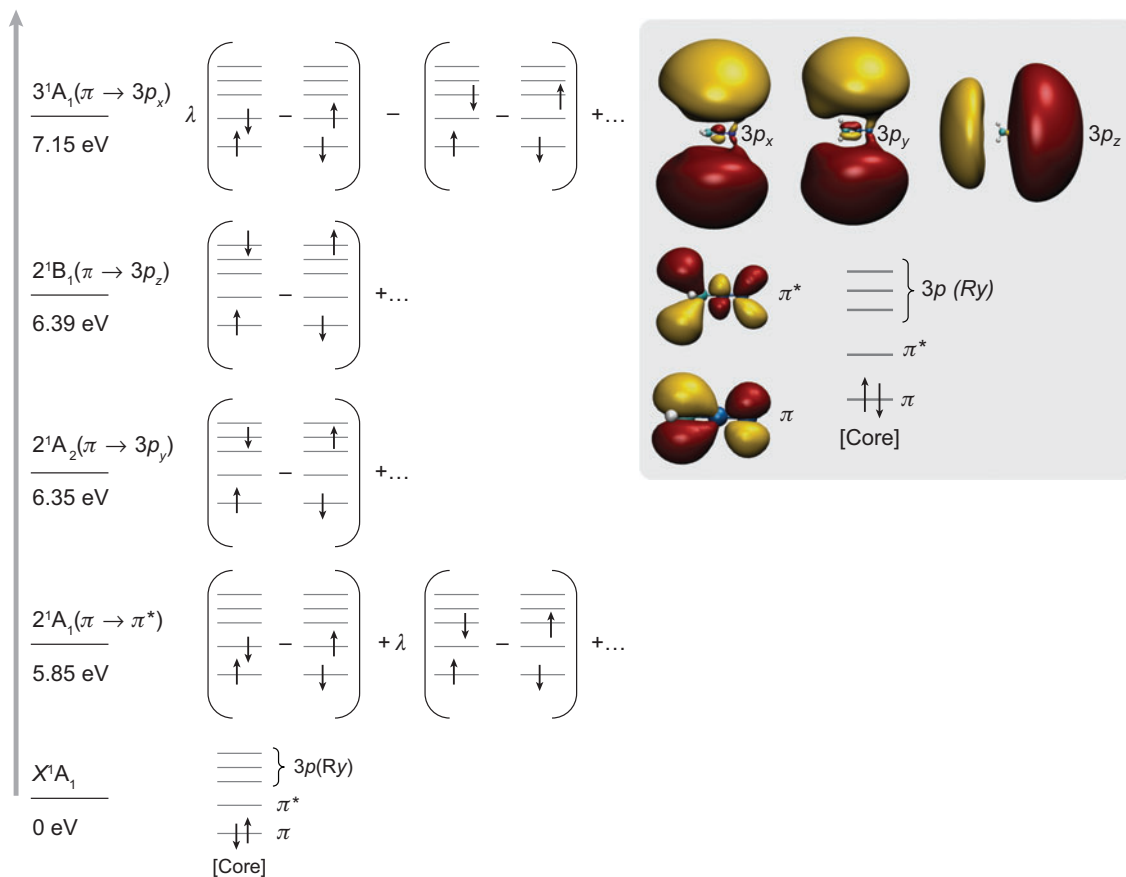


**Figure 1**

The molecular orbitals and electronic configurations of the low-lying singlet valence and Rydberg excited states of diazomethane.

time-dependent density-functional theory would fail, owing to a self-interaction error that spoils the description of Rydberg (and charge-transfer) states.

Rydberg–valence interactions are ubiquitous in both closed-shell molecules and radicals (44–49) and have an important effect on potential-energy-surface (PES) shapes (46, 48), spectroscopy, and dynamics (44, 46–48). They exemplify a more general effect—mixing between states of different character (e.g., mixing of  $n \rightarrow \pi^*$  and  $\pi \rightarrow \pi^*$  configurations in nuclear bases at deformed geometries and interplay between covalent and zwitterionic states).

Finally, although point-group symmetry may be exploited in EOM calculations (e.g., by diagonalizing  $\bar{H}$  in different symmetry blocks), the EOM description of the excited states is uniform for the states of the same or different symmetry. Thus, the “excited states of the same symmetry as the ground state” problem does not exist in EOM.

**3.1.2. EOM for exactly and nearly degenerate states: complicated Jahn-Teller intersection in cyclic  $N_3^+$ .** Cyclic  $N_3^+$  is a closed-shell molecule with doubly degenerate HOMO and doubly degenerate lowest unoccupied molecular orbital (LUMO) (50–52). Thus, HOMO  $\rightarrow$  LUMO excitations give rise to a manifold of four singlet and four triplet states (50). Symmetry analysis reveals that two of the states (in each manifold) are exactly degenerate at  $D_{3h}$  and thus should form a JT pair. However, the presence of two other nearly degenerate states makes the intersection complex. A similar excited-state pattern is present in other molecules when both HOMO and LUMO are doubly degenerate (e.g., benzene or 1,3,5-triazine).

**Figure 2** shows EOM-EE PES scans along the bending coordinate and electronic configurations of the four lowest singlet excited states. Note that all four states get scrambled as one passes the intersection. The intersection appears glancing rather than conical (see **Figure 2b,c**); however, as shown by Dillon & Yarkony (52), this results from the close proximity of three additional conical intersections, which become obvious as one further zooms in (see **Figure 2d**). EOM-EE accurately reproduces exact and near degeneracies, as well as changes in electronic wave functions around the intersection, in this challenging system regardless of how many EOM states are computed.

The flexibility of the EOM wave functions and its ability to describe the mixing of states of different character are responsible for the proper formal structure of EOM-EE response functions necessary to describe vibronic interactions or pseudo-JT effects (18, 53). Thus, EOM is attractive for studying JT systems, vibronic

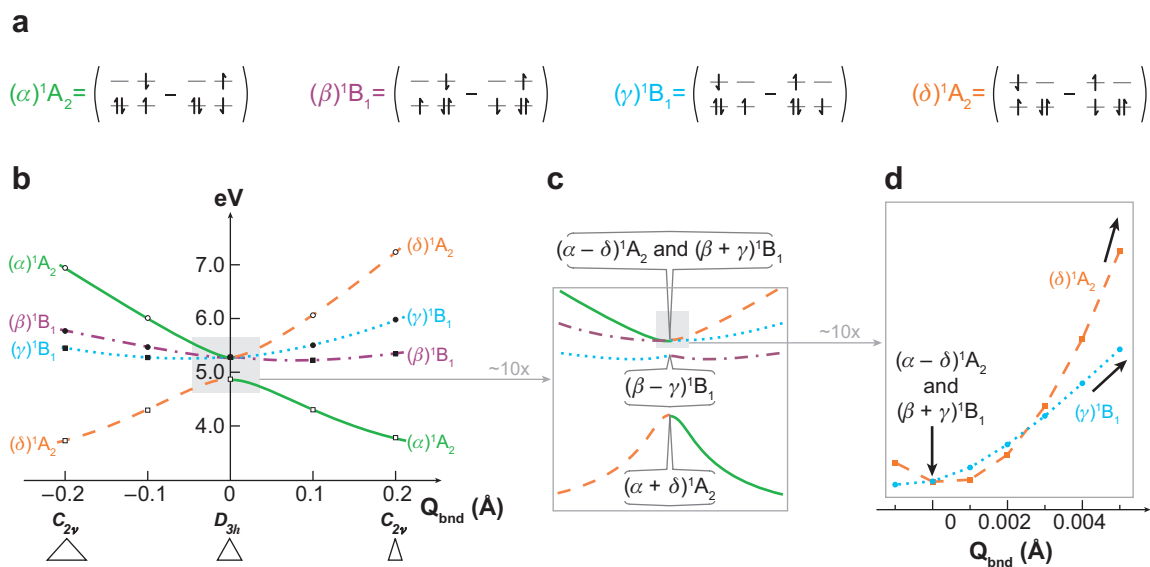


**Figure 2**

Electronic configurations (a) and potential-energy-surface scans of increased resolution (b–d) of the four singlet HOMO  $\rightarrow$  LUMO excited states of cyclic  $N_3^+$ .

interactions, and conical intersections (54–58), although special care (59) should be taken for the conical intersections between states of the same symmetry owing to its non-Hermitian nature, which results in complex eigenvalues in the vicinity of the intersection and, therefore, violates its topology (59, 60).

**3.1.3. EOM-EE for excited states of doublet radicals: vinyl and beyond.** EOM-EE can employ open-shell (e.g., doublet) references. **Figure 3** shows the MOs of vinyl radical and the set of singly excited determinants generated by  $R^{EE}$  from this reference. Note that the transitions unique to radicals (that is, those involving half-filled orbitals) form a spin-complete set. Thus, EOM-EE describes these states with an accuracy similar to that of closed-shell applications, provided there is no strong spin contamination in the reference. The set of determinants that involves other transitions (e.g.,  $\pi \rightarrow \pi^*$  and  $\pi \rightarrow Ry$ ) is not spin complete, and the missing configurations appear as double excitations (61). Because doubles are present in EOM-EE-CCSD, the EOM description of these states is not as disastrous as by CI with single substitutions (62); however, it is still lacking (61). Fortunately, these states are often higher in energy than the first group. In the vinyl and related family of unsaturated hydrocarbon radicals (49), however, such states are important, and we have employed EOM-SF to improve their description.

Chemists are often interested in understanding systematic trends in homologous series, for example, how excited states localized on a chromophore would be affected by different substitutions. We addressed this question for the family of unsaturated hydrocarbon radicals derived from vinyl (49). Although all low-lying states in these radicals retain their vinyl-like character (see **Figure 3**), their excitation energies

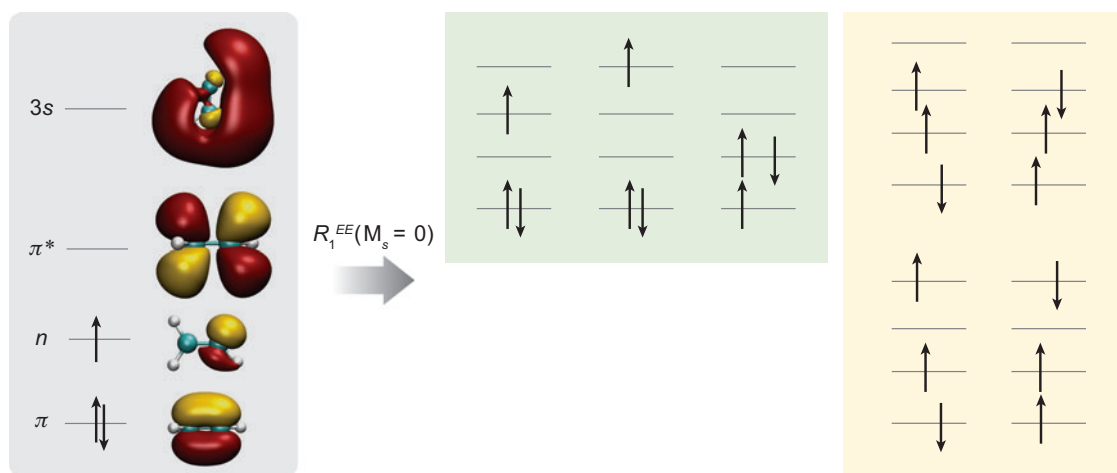


**Figure 3**

The molecular orbitals and the electronic configuration of the ground state of vinyl and the determinants generated by spin-conserving single excitations. The set of determinants involving transitions between half-filled orbitals ( $n \rightarrow \pi^*$ ,  $n \rightarrow Ry$ ,  $\pi \rightarrow n$ ) is spin complete. The second set that involves ethylene-like transitions is not spin complete.



exhibit an interesting behavior—the valence states remain essentially unaffected by the hydrocarbon chains, whereas the excitation energies of the Rydberg states decrease systematically with radical size following the decrease in ionization energies. The code for properties calculations (transition dipoles and second moments) was crucial in assigning the states' characters.

This type of study requires a method whose accuracy is not affected by the molecule's size. In the context of our example, the excitation energies of the chromophore (i.e., vinyl) should not be affected by the presence of any number of other closed-shell molecules at infinite distance. This property (size intensivity) is closely related to size consistency and is rigorously satisfied for EOM-EE energies (23, 31, 32; see also footnote 32 in Reference 19). It ensures a uniform quality for the results for different size molecules. However, not all EOM properties are size intensive, which is a primary motivation for employing alternative linear-response formalism (33, 34).

### 3.2. EOM for Diradicals, Triradicals, and Bond Breaking: The Spin-Flip Route

When target states are multiconfigurational owing to orbital degeneracies, one can choose a high-spin reference. To obtain target low-spin states, the EOM operators should include SF, giving rise to the EOM-SF family (10, 19, 42). So far, models based on a high-spin triplet and quartet references have been implemented and benchmarked (10, 19, 39, 42, 63–67); however, extensions of the SF approach to higher spin references are also promising.

An attractive feature of the triplet and quartet reference-based EOM-SF models is that only a single SF is required to obtain target  $M_s = 0$  or  $M_s = \frac{1}{2}$  states. That is why the corresponding EOM-SF equations in a spin-orbital form are identical to the EOM-EE equations, which greatly simplifies the implementation.

The target low-spin states are described as spin-flipping excitations:

$$\Psi_{M_s=0}^{s,t} = R_{M_s=-1} \Psi_{M_s=+1}^t, \quad (8)$$

$$\Psi_{M_s=1/2}^{d,q} = R_{M_s=-1} \Psi_{M_s=+3/2}^q, \quad (9)$$

where  $\Psi_{M_s=+1}^t$  and  $\Psi_{M_s=+3/2}^q$  are the high-spin components of the triplet and quartet states, respectively.  $\Psi_{M_s=0}^{s,t}$  denotes the target open- and closed-shell singlet and triplet states, and  $\Psi_{M_s=1/2}^{d,q}$  represents the low-spin doublets and quartets. The operator  $R_{M_s=-1}$  is an excitation operator that flips the spin of an electron:

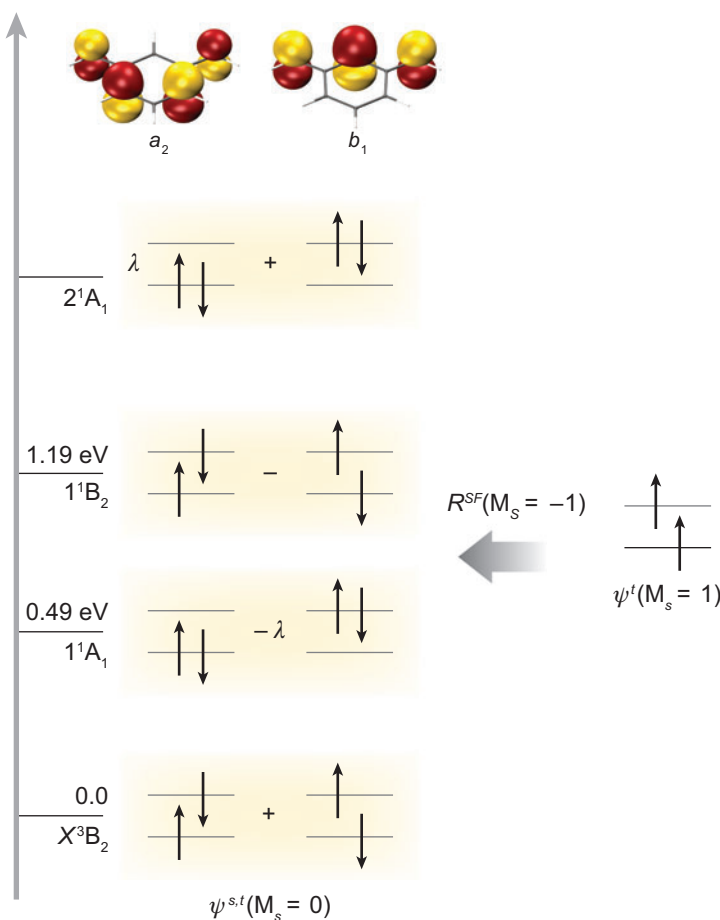
$$R_{M_s=-1} \equiv R^{SF} = \sum_{ia} r_i^a a_\beta^\dagger i_\alpha + \dots \quad (10)$$

As demonstrated below, all the configurations needed to describe diradical- or triradical-type wave functions are formally single excitations with respect to the corresponding high-spin references. The ability of SF to tackle diradical states can be exploited to describe bond breaking (42, 68). For example, the PES along  $\sigma$ -bond breaking can be accurately described by EOM-SF using a  $^3\sigma\sigma^*$  reference. Similarly, the torsional potential around a double bond (e.g., twisted ethylene) can be described by EOM-SF using a  $^3\pi\pi^*$  reference.

**3.2.1. Substituted meta-xylylene diradicals: EOM-SF for two electrons in two orbital systems.** Figure 4 shows frontier MOs and electronic configurations of the four  $M_s = 0$  diradical states of meta-xylylene (MX). The high-spin  ${}^3B_2$  state, which is well described by a single determinant, is used as the reference,  $\Psi_{M_s=+1}^t$  of Equation 9, for SF calculations. The spin-flipping EOM operator,  $R^{SF}$ , generates all four  $M_s = 0$  determinants necessary to describe two closed-shell diradical singlet states,  $1^1A_1$  and  $2^1A_1$ , as well as the open-shell singlet  $1^1B_2$  state and the  $M_s = 0$  component of the triplet. In SF calculations, we calculate energy spacings between the states with respect to the latter, whereas the high-spin state (which has slightly different energy because it is parameterized somewhat differently than its high-spin partner in this approach) just serves as the reference. All four states are treated by SF on an equal footing, and their varied two-configurational character is easily described by EOM-SF. This balanced description is responsible for error cancellation that results in accurate energy separations (e.g., singlet-triplet gaps) at a relatively

**Figure 4**

Frontier molecular orbitals of meta-xylylene and the electronic configurations of the four  $M_s = 0$  diradical states. Spin-flip calculations are using  $\alpha\alpha$  triplet reference,  $\Psi^t(M_s = 1)$ . Adiabatic energy separations are shown.



low level of correlation (67). Note that dynamical correlation is included simultaneously with the nondynamical one, which results in a single-step computational scheme and, therefore, avoids the intruder-state problem. Thus, the multiconfigurational character of the wave function, the optimized geometries, frequencies, and other properties calculated with EOM-SF-CCSD are more accurate than the bare multiconfigurational self-consistent-field values (69).

The ground state of MX is triplet, which is why this molecule attracted considerable interest as a model system for molecular magnets. The closed-shell singlet is approximately 0.5 eV higher in energy (adiabatically). One important practical question is how this energy gap depends on substituents. The SF methodology is particularly appropriate to address this question computationally because of its multistate nature and size consistency (see Section 3.1.3), which enable uniform applications to series of molecules and dense manifolds of states. This is demonstrated in **Figure 5**, which shows a series of substituted MX diradicals and their vertical state orderings (70).

**3.2.2. EOM-SF for dense manifolds of electronic states in triradicals.** Although triradicals (molecules with three unpaired electrons) feature even more extensive degeneracies than diradicals, their SF description is just as simple and straightforward (57, 71–77). Using high-spin quartet reference (see Equation 9), one can access all the multiconfigurational triradical states through single SF excitations, as evident from **Figure 6**, which shows vertical state ordering in three related triradicals: 5-dehydrometaxylene (5-DMX), 2-DMX, and 1,3,5 trimethylenebenzene. In these systems with such large density of states (e.g., 5-DMX has seven states under 3.5 eV), the multistate nature of EOM-SF as well as the simultaneous inclusion of dynamical and nondynamical correlation were crucial in the studies of relative state ordering and the nature of the ground state in triradicals.

### 3.3. EOM for Ionized or Electron Attached States, Doublet Radicals, and Charge-Transfer Systems: EOM-IP and EOM-EA

EOM excitations can also change the number of electrons in the system, which is the essence of the EOM–ionization potential (IP) or EOM–electron affinity (EA) methods (11–14). The reference states for EOM-IP/EA are determinants for  $N + 1$  /  $N - 1$  electron states, whereas the final states are  $N$  electron ones.

One can employ these methods to calculate ionization energies or electron affinities. Another class of less obvious but successful applications of the EOM-IP/EA methods is not concerned with electron ionization or attachment processes, but rather targets ground and excited states of problematic open-shell systems. These applications use an  $N - 1$  or  $N + 1$  electron reference state to generate a balanced set of configurations needed for a target  $N$  electron system. For example, to avoid the troublesome symmetry breaking in doublet radicals (or to obtain spin-pure wave functions), EOM-IP/EA methods have been successfully applied (13, 55, 58, 78). In these models, the reference determinant is judiciously chosen to represent a closed-shell cation or anion, and the EOM operators do not conserve the number

---

**IP:** ionization potential

**EA:** electron affinity

---

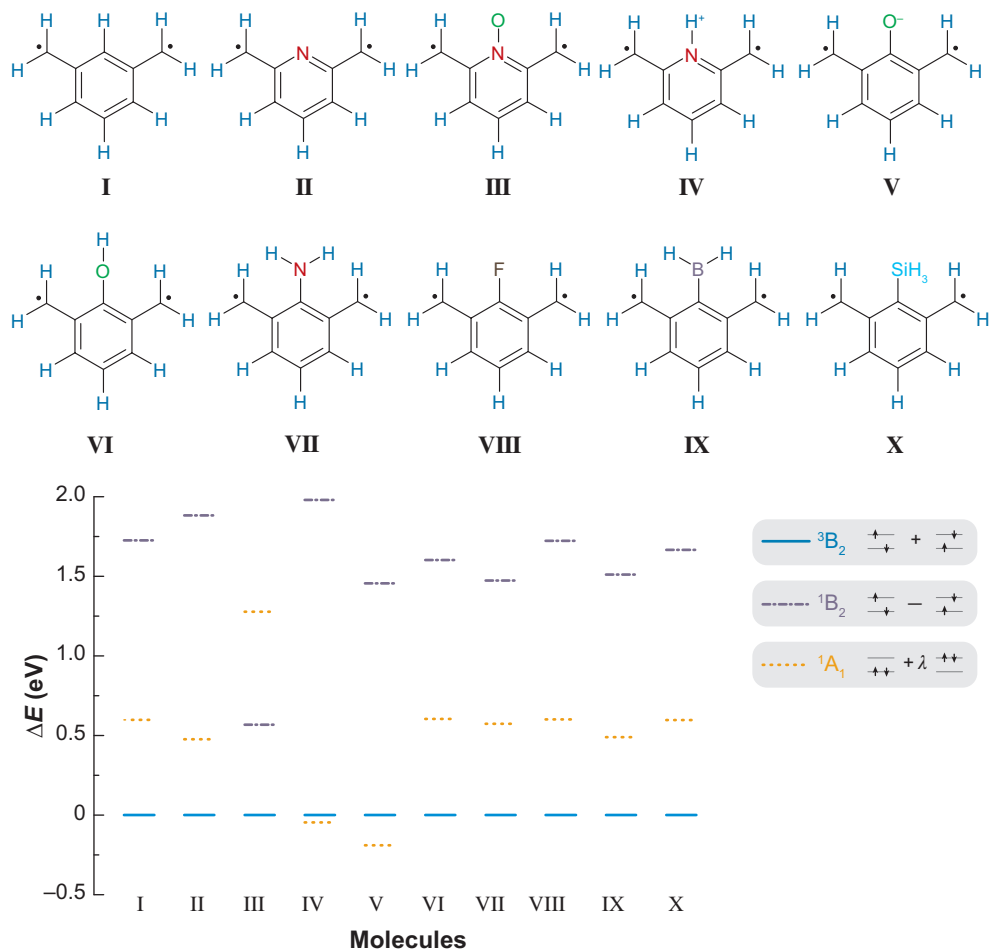


**Figure 5**

Substituted meta-xylylene diradicals (*upper panel*) and their vertical state ordering (*lower panel*). The singlet-triplet gaps are surprisingly insensitive to the substituent electronegativities, as well as their  $\sigma$  or  $\pi$  donor-acceptor properties, while introducing the charge results in the reversal of states ordering (the adiabatic gaps are of course even larger). Note an interesting effect resulting from NO substitution—the dramatic stabilization of the open-shell singlet state.

of electrons (11–14):

$$R^{IP} = \sum_i r_i i + \dots, \quad (11)$$

$$R^{EA} = \sum_a r_a a^+ + \dots, \quad (12)$$

which, in other words, are of  $b$ ,  $2bp$ ,  $\dots$  and  $p$ ,  $b2p$ ,  $\dots$  type.

EOM-IP/EA is the method of choice for charge-transfer systems (79, 80) in which charge localization patterns are determined by the interaction between two electronic

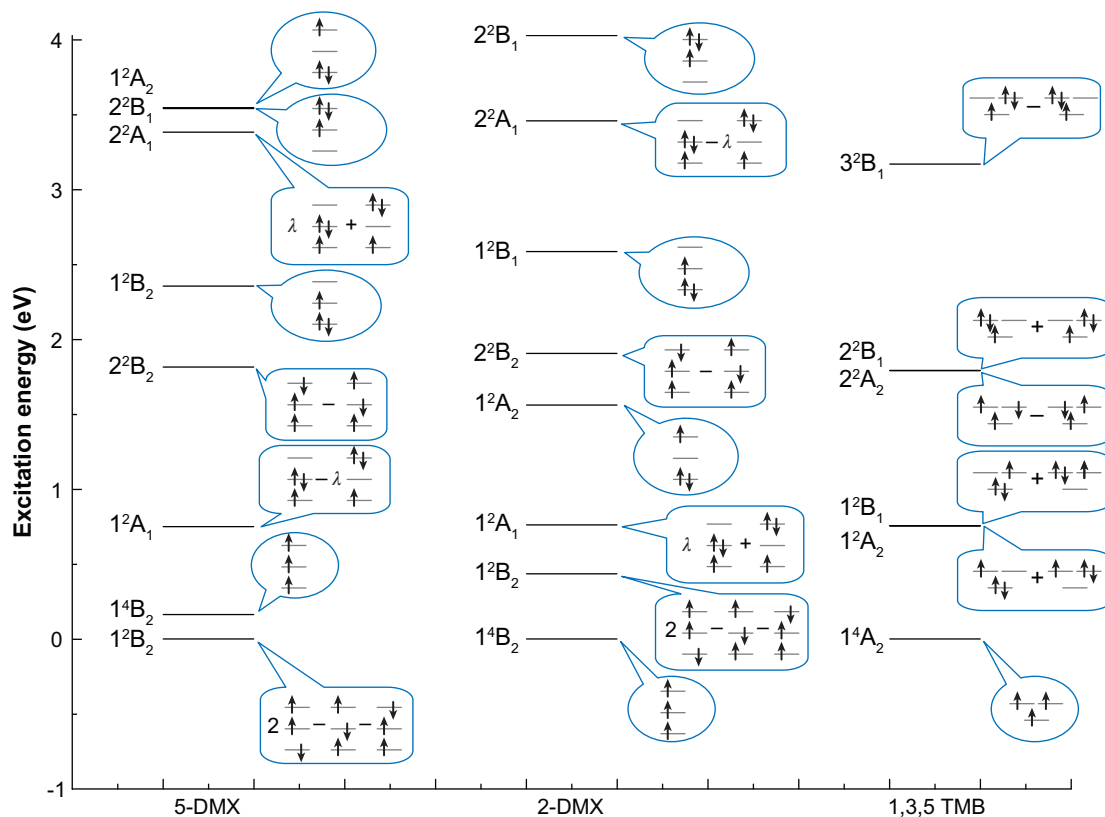


**Figure 6**

Vertical state ordering in 5-dehydrometaxylene (5-DMX), 2-DMX, and 1,3,5 trimethylenenebenzene (TMB) at the corresponding equilibrium geometries. 2-DMX and 1,3,5 TMB have a quartet ground state (in accordance with Hund's rule); however, 5-DMX features an open-shell doublet electronic configuration, an unusual pattern for an organic molecule.

states. Recent benchmarks on small ionized noncovalent dimers (80) demonstrated that EOM-IP yields accurate PESs and diabatic couplings for charge-transfer processes and, more importantly, properly describes charge localization. The latter was found to be surprisingly difficult to describe by single-reference methods using open-shell doublet references, even at a highly correlated level. For example, CCSD calculations of three-electron systems such as  $(\text{He})_2^+$  and  $(\text{H}_2)_2^+$  yield incorrect asymptotic behavior and overlocalize the charge. The advantages of the EOM-IP method become even more important when the ionized states of the monomers feature electronic degeneracies, as in benzene dimer cation (81) discussed below.

**3.3.1. EOM for charge-transfer and extreme degeneracies: bonding and charge localization patterns in 10 electronic states of the benzene dimer cation.** Figure 7 shows the MOs and electronic states of the ionized benzene dimer (81), a model system for ionized  $\pi$ -stacked aromatic molecules. Because of pairs of

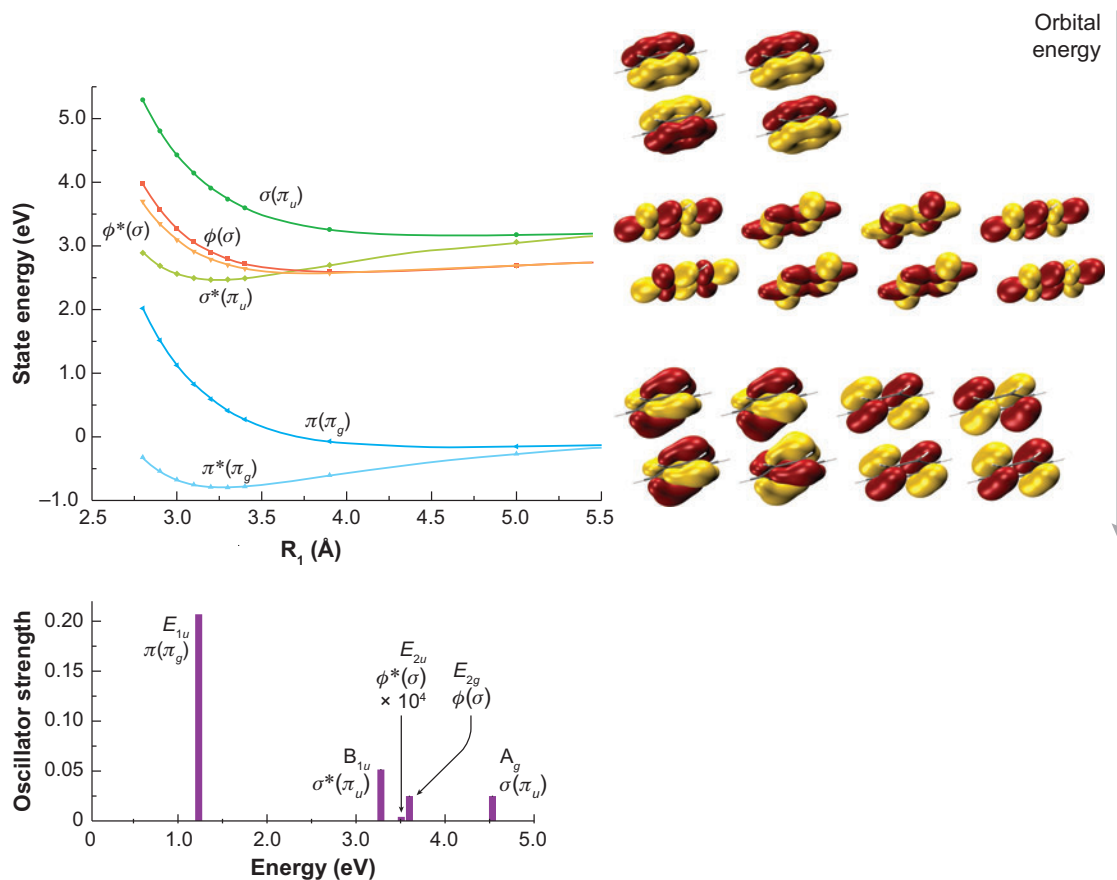


**Figure 7**

Molecular orbitals, potential energy curves, and the electronic stick spectrum for the benzene dimer cation. Note the intense charge-resonance transition at approximately 1.3 eV.

degenerate MOs that give rise to pairs of JT states in the cation, even the ionized benzene monomer is a challenging system. Calculations employing open-shell doublet reference fail to reproduce the JT degeneracy and are spoiled by spin contamination. Moreover, this also complicates the description of the excited states of the cation (i.e., those derived by ionizations from HOMO-1 and HOMO-2 orbitals). In the dimer, which features 10 low-lying electronic states, the situation is even more complex.

EOM-IP elegantly and effortlessly overcomes all the above challenges. The calculations employ a well-behaved closed-shell neutral reference, and the target states are accessed through Koopmans-like excitation operators (see Equation 11). The resulting doublet wave functions are naturally spin adapted. All leading configurations for the 10 states appear at the same excitation level, which allows the accurate description of state interactions at lower-symmetry geometries, as well as charge flow along the charge-transfer coordinate (80). Finally, calculations of electronic transitions in the

cation are possible, as demonstrated by the stick electronic spectrum of the lowest-energy isomer in **Figure 7**. An interesting and important feature of these systems is the appearance of intense charge-resonance transitions that are unique to the ionized dimers and very sensitive to the geometries, which suggest their exploitation in experimental studies of charge localization dynamics.

### 3.4. EOM-DIP and Beyond

The nonparticle conserving approach can be taken even further—as in the double ionized EOM model (EOM-DIP) (40, 41), in which the excitation operators are of  $2b, 3b1p, \dots$  type. The initial benchmark examples included benzyne (82) and ozone (41), for which doubly attached dianion references have been employed. Although these types of wave functions are easily accessible by EOM-SF, the computational cost of EOM-DIP is lower, and the target wave functions are naturally spin adapted. Unfortunately (see Section 5), the performance of the straightforward implementation of EOM-DIP has been found unsatisfactory owing to strong orbital-relaxation effects and the physical instability of the doubly attached references. Hopefully, future developments will resolve this problem, as the method offers an elegant solution for more sophisticated diradicals (e.g.,  $\text{CH}_2\text{CH}_2\text{O}$  or O-Rg complexes), in which the low-lying states are of four-electrons-in-three-orbitals type and are, therefore, not well described by EOM-SF.

## 4. FORMALISM: A DEEPER VIEW

On no account allow a Vogon to read poetry at you.

*The Hitchhiker's Guide to the Galaxy*, Douglas Adams

This section presents an abridged formal derivation of EOM-CC equations, which emphasizes the similarities with earlier EOM methods (83) and variational properties of EOM-CC (see Reference 10 for a more detailed version). For example, we do not invoke the projective approach (9) and demonstrate that the killer condition is rigorously satisfied in single-reference EOM-CC theories.

Let us consider a general (not necessarily Hermitian) operator  $\tilde{H}$  and two of its eigenstates,  $|0\rangle$  and  $|f\rangle$ , with eigenvalues  $E_0$  and  $E_f$ , respectively:

$$\tilde{H}|0\rangle = E_0|0\rangle, \quad (13)$$

$$\tilde{H}|f\rangle = E_f|f\rangle. \quad (14)$$

For a non-Hermitian operator, bra eigenstates are not Hermitian conjugates of ket eigenstates,  $\langle k| \neq (|k\rangle)^+$ , and neither bra nor ket eigenstates form an orthonormal set. However, they form a biorthogonal set,  $\langle k|l\rangle = \delta_{kl}$ , provided that the corresponding eigenvalues are nonzero. A general excitation operator  $R(f)$  is defined such that it promotes a system from the initial (or reference) state  $|0\rangle$  into the final state  $|f\rangle$ :

$$R(f)|0\rangle = |f\rangle. \quad (15)$$

No assumptions are made about the nature of the initial and final states: They can be the ground and electronically excited states (or any two electronic states) of an  $N$  electron system, or states of an  $N$  electron and an ionized or detached system, and so on. It is convenient to represent the excitation operator  $R$  from Equation 15 by the following bra-ket form:

$$R(f) \equiv |f\rangle\langle 0|. \quad (16)$$

The so-defined operator can act on any reference state  $|\tilde{0}\rangle$ :

$$R(f)|\tilde{0}\rangle = |f\rangle\langle 0|\tilde{0}\rangle. \quad (17)$$

Therefore, for any state  $|\tilde{0}\rangle$  that has a nonzero overlap with the exact reference state  $\langle 0|$ ,

$$[\bar{H}, R(f)]|\tilde{0}\rangle = \omega_{of} R(f)|\tilde{0}\rangle, \quad (18)$$

where  $[\bar{H}, R(f)] = \bar{H}R(f) - R(f)\bar{H}$ , and  $\omega_{of} = E_f - E_0$ . The above equation shows that if no approximations have been made for the excitation operator  $R(f)$ , one can compute the exact energy difference  $\omega_{of}$  without an explicit calculation of the initial and final states.

By introducing the de-excitation operator  $L(f) = |0\rangle\langle f|$ , we can write the transition energy  $\omega_{of}$  as a general expectation value of the non-Hermitian operator  $\bar{H}$ :

$$\omega_{of} = \frac{\langle \tilde{0}|L(f)[\bar{H}, R(f)]|\tilde{0}\rangle}{\langle \tilde{0}|L(f)R(f)|\tilde{0}\rangle}. \quad (19)$$

It is convenient to choose the bra reference state  $\langle \tilde{0}|$  to be a Hermitian conjugate of the ket reference state. Equation 19 provides a useful functional whose stationary values coincide with the eigenvalues of Equation 18 when the operator  $R(f)$  is represented in a complete operator basis set. However, the corresponding  $\omega$ 's do not provide upper bounds of the exact energy differences, even when a Hermitian operator (i.e., the bare Hamiltonian  $H$ ) is used in Equation 19, and the de-excitation operator is a Hermitian conjugate of the excitation operator [in this case, the corresponding total energies are upper bounds of the exact total energies given that a linear parameterization of the excitation operator  $R(f)$  is used (84)].

One can consider alternative functionals (83, 85, 86) that would yield results identical to Equation 19 in the complete operator basis-set limit, or when the so-called killer condition is satisfied (83):

$$L(f)|\tilde{0}\rangle = 0. \quad (20)$$

The killer condition means that the reference state  $|\tilde{0}\rangle$  cannot be de-excited (i.e., the reference can be regarded as a vacuum). Alternatively, Equation 20 can be interpreted as orthogonality of the reference and final states:

$$L(f)|\tilde{0}\rangle = |0\rangle\langle f|\tilde{0}\rangle = 0. \quad (21)$$

The killer condition (Equation 21) is satisfied when (a) the exact initial state is used as the reference and the operator basis is complete with respect to the final states, or (b) the single Slater determinant is used as the reference  $|\tilde{0}\rangle$ , and the operator  $L$  is pure de-excitation operators with respect to the reference  $|\tilde{0}\rangle$  (i.e., does not



annihilate electrons from the occupied orbitals and does not create electrons in the virtual orbitals).

At this point, we depart from the textbook EOM presentation (83). Instead of general excitation operators  $R(f)$ ,  $L^+(f)$ , which generate the exact final state  $|f\rangle$  when acting on any reference state provided that  $\langle 0|\tilde{0}\rangle \neq 0$ , we introduce less general operators  $\tilde{R}(f)$ ,  $\tilde{L}^+(f)$  defined with respect to the specific reference  $|\tilde{0}\rangle$ :

$$\begin{aligned}\tilde{R}(f) &= |f\rangle\langle\tilde{0}|, \\ \tilde{L}(f) &= |\tilde{0}\rangle\langle f|.\end{aligned}\tag{22}$$

Unlike  $R(f)$ ,  $\tilde{R}(f)$  does not yield the exact final state when acting on a state  $|g\rangle$  with nonzero overlap with  $|0\rangle$  if  $\langle\tilde{0}|g\rangle = 0$ :  $\tilde{R}(f)|g\rangle = |f\rangle\langle\tilde{0}|g\rangle = 0$ . Because commutator Equation 18 is no longer valid for  $\tilde{R}$  (unless, of course, the reference  $|\tilde{0}\rangle$  happens to be the exact eigenstate  $|0\rangle$ ), the EOM functionals do not yield the exact  $\omega_{of}$  even when the operators  $\tilde{R}(f)$  and  $\tilde{L}^+(f)$  are expanded over the complete basis. However, the difference between the resulting  $\omega_{of}$  and the exact one assumes the same constant value for all the target states  $|f\rangle$  (see footnote 24 in Reference 10). Therefore, for an arbitrary reference  $|\tilde{0}\rangle$ , the exact energy gap between any two target states  $|f\rangle$  and  $|i\rangle$  is retrieved from Equation 19 in the limit when the operators  $\tilde{R}(f)$  and  $\tilde{L}^+(f)$  are expanded over the complete basis.

In practice, excitation and de-excitation operators are expanded over a finite basis set. It is convenient to employ linear parameterization and expand the excitation and de-excitation operators over a set of operators  $\rho_k$  and  $\lambda_k$ :

$$\tilde{R}(f) = \sum_k r_k^f \rho_k,\tag{23}$$

$$\tilde{L}(f) = \sum_k l_k^f \lambda_k.\tag{24}$$

When acting on the reference  $|\tilde{0}\rangle$ , these operators generate a biorthogonal set of basis functions, and the completeness of the operator basis set  $\{\rho_k, \lambda_l\}$  is derived from the completeness of the Hilbert space spanned by these functions. Only the completeness with respect to the target states  $|f\rangle$  is required for the EOM functionals to yield the exact energy differences between the target states, whereas the Hilbert space can be incomplete with respect to other groups of eigenstates, provided that the target states are not interacting across the Hamiltonian with these groups (e.g., states of different point-group or spin symmetry, or with a different number of electrons).

By considering the first variation of the functional from Equation 19 with respect to right  $\tilde{R}$  and left  $\tilde{L}$  vectors, and assuming that variations  $\delta\tilde{R}$  and  $\delta\tilde{L}$  are independent, we arrive at a non-Hermitian secular problem for the expansion coefficients  $\{r_k\}$  and  $\{l_k\}$ :

$$(\tilde{\mathbf{H}} - E_0)\mathbf{R} = \mathbf{R}\mathbf{\Omega},\tag{25}$$

$$\mathbf{L}(\tilde{\mathbf{H}} - E_0) = \mathbf{\Omega}\mathbf{L},\tag{26}$$

$$E_0 = \langle\tilde{0}|\tilde{H}|\tilde{0}\rangle,\tag{27}$$

where matrices  $\mathbf{R}$  and  $\mathbf{L}$  are constructed from the expansion coefficients  $\{r_k\}$  and  $\{l_k\}$  from Equations 23 and 24; the diagonal matrix  $\mathbf{\Omega}$  contains the transition energies,

$\Omega_{kk} = \omega_{0k}$ ; and  $\tilde{\mathbf{H}}$  is the matrix of the Hamiltonian operator  $\tilde{H}$  in the basis of configurations generated by  $\{\rho_k, \lambda_l\}$  from the reference  $|\tilde{0}\rangle$ .

At this point, we can specify the reference  $|\tilde{0}\rangle$ , Hamiltonian  $\tilde{H}$ , and the operator basis  $\rho_k, \lambda_k$ , which define an EOM model. The first applications of the EOM formalism used the bare Hamiltonian  $H$  and employed correlated (e.g., MR) wave functions as the reference state  $|\tilde{0}\rangle$  (6, 87). By analogy, the first applications of the EOM formalism to the CC models also used the bare Hamiltonian (e.g., 22, and references therein) and the CC wave function (35) as the reference  $|\tilde{0}\rangle$ . In this approach, the killer condition (Equation 20) is not satisfied, which makes the choice of an EOM functional rather arbitrary. Even more disturbing, a straightforward application of Equation 19 does not yield EOM-CC equations even if one replaces the bra reference by  $\langle\Phi_0|\exp(-T)$  as opposed to  $\langle\Phi_0|\exp(T^+)$ . That is why a projective approach has been traditionally used to derive the EOM equations (7, 9, 22), although variational properties of the EOM-CC theory have been recognized (9, 88).

Alternatively, we chose  $\tilde{H}$  to be the similarity transformed Hamiltonian, and a single Slater determinant  $|\Phi_0\rangle$  as the reference state  $|\tilde{0}\rangle$ , which greatly simplifies the choice of the excitation operators  $\tilde{R}$ ,  $\tilde{L}^+$ , and easily satisfies the killer condition (Equation 20), although, in Surján terms, for the wrong reason (89). This immediately retrieves the single-reference EOM-CC equations from Section 2, where  $\tilde{R}$  and  $\tilde{L}^+$  are denoted as  $R$  and  $L$ .

Regardless the nature of  $T$ , similarity transformation does not change the eigenvalues of the Hamiltonian—therefore, stationary values of Equation 19 yield exact energy differences between the target states when the excitation operators  $\tilde{R}$  and  $\tilde{L}^+$  are expanded over the complete operator basis set. However, the exact  $\omega_{of}$  can only be obtained when both the operator set is complete and  $|\tilde{0}\rangle \equiv |0\rangle$ . The latter can be achieved by an appropriate choice of  $T$  from the similarity transformation (i.e., when  $T$  is not truncated and satisfies the CC equations for the reference  $|\tilde{0}\rangle$ ), the single determinant  $|\tilde{0}\rangle$  becomes an eigenstate of  $\tilde{H}$ .

For example, although EOM-IP/EA-CC yields the exact ionization energies/EA only under the same conditions as EOM-EE-CC, we can achieve the exact description of the target (ionized or attached) states with only the EOM operators expanded over the complete basis. For instance, the EOM-IP-CC description of the lithium atom is exact even with  $T = 0$ , provided that  $R$  includes up to  $4b3p$  excitations.

## 5. KNOWING YOUR WAY AROUND IN FOCK SPACE: LIMITATIONS, CAVEATS, AND SHORTCUTS

He knew where his towel was.

*The Hitchhiker's Guide to the Galaxy*, Douglas Adams

For any EOM model, the quality of the target-state wave functions depends on two factors. First, the reference state should be well described within a single-reference CC approach; that is, a single Slater determinant should provide a qualitatively correct zero-order wave function. Second, the leading configurations in the target wave functions should appear at the same excitation level. For EOM-EE, both conditions

are easily satisfied for singly excited states of closed-shell molecules around their ground-state equilibrium geometries. A large HOMO-LUMO gap results in a single-configurational ground state and low-lying excited states that are of singly excited character. Similarly, excited states of doublet radicals dominated by excitations to or from half-filled orbitals are reasonably well described provided the reference spin contamination is moderate or, better yet, spin-restricted reference is employed.

If, however, the reference state acquires considerable multiconfigurational character (as, for example, happens along a bond-breaking coordinate, in diradicals, transition metals, and other cases with small HOMO-LUMO gaps), the quality of the CC ground-state wave functions deteriorates, resulting in less accurate excitation energies. For example, in the extreme case of a molecule with a completely broken  $\sigma$ -bond, EOM-EE yields a negative excitation energy for the  ${}^3\sigma\sigma^*$  state, which, in fact, is degenerate with the ground state.

Nevertheless, even when the reference state is heavily multiconfigurational, some target EOM states may still be well described, provided that single excitations from the reference determinant produce all the leading configurations for the target states. For example, the open-shell  $\pi\pi^*$  singlet state of ethylene is well described by EOM-EE both at equilibrium, where the ground-state wave function is dominated by the single determinant,  $(\pi)^2$ , and at the barrier, where the reference-state wave function becomes two-configurational,  $(\pi)^2 - (\pi^*)^2$ . Moreover, the energy differences between the target EOM states may be reproduced rather accurately (as follows from the formal properties of EOM discussed in the previous section), even when the reference state is multiconfigurational and the absolute excitation energies are poor. For example, despite the diradical character of the reference singlet  $\tilde{a}^1A_1$  state, the  $\tilde{a}^1A_1 - X^3B_1(M_x = 0)$  energy gap in methylene is within 0.055 eV of the full CI value, and the error in the  $\tilde{b}^1B_1 - X^3B_1(M_x = 0)$  energy difference is even smaller, 0.024 eV (67). This allowed successful applications of EOM-EE to such a challenging multiconfigurational system as the NO dimer (47, 48).

A small HOMO-LUMO gap also results in an increased doubly excited character in some of the states, as well as low-lying states dominated by double excitations. Even though doubly excited determinants are formally present in EOM-CCSD wave functions, the EOM description of these states is disastrous because the important configurations appear at a different excitation level and, therefore, are not treated in a balanced fashion. Good examples of this type include the second closed-shell singlet state of methylene ( $\tilde{c}^1A_1$ ), the Z-state in twisted ethylene, the doubly excited dark states in polyenes, and infrared excited states in the NO dimer. Similar effects—leading configurations appearing at different excitation levels—are responsible for a less accurate description and increased spin contamination of the excited states in doublet radicals dominated by excitations from doubly occupied to virtual orbitals.

EOM-EE should be used with caution (if at all) when the reference state is exactly degenerate, even if the reference wave function is single configurational owing to symmetry constraints. For example, one of the two components of the doubly degenerate  $\Pi$  ground state of the OH radical is well described by CCSD. The EOM-EE-CCSD calculation from this reference yields a reasonably accurate description of some excited states, but not of the second component of the ground state, which

appears at nonzero excitation energy. Similarly, JT degeneracies are not reproduced if the calculations are set up using one of the degenerate components as the reference because within such a framework of the calculation, the two states appear at a different excitation level (one versus zero) and therefore are not treated in a balanced way.

Although spin contamination of CCSD wave functions for open-shell references is usually quite small (90, 91), the EOM target states are much more sensitive. It appears that restricted open-shell Hartree-Fock references yield consistently better results than unrestricted Hartree-Fock, both for EOM-EE from doublets and for EOM-SF from triplets and quartets. In some cases (56), optimized-orbital CCD (92, 93) produced the best results.

However, even when using spin-pure reference, the target SF states exhibit small spin contamination, as all single and double excitations from an open-shell reference do not form a spin-complete set (additional spin contamination is present owing to the exponential form of the cluster operator). Although this residual spin contamination is rather small, it is desirable to implement spin-adapted versions of EOM-SF/EE to improve accuracy (65).

With regard to bond-breaking applications of EOM-SF, enforcing the proper reference along the entire PES might be difficult if the desired triplet state is not the lowest triplet (68). Finally, SF excitations fail to yield a balanced set of determinants necessary to describe all low-lying states when orbital degeneracies are more extensive, for example, as in a Be atom (two electrons in three orbitals) (42) or in O-He (four electrons in four orbitals).

With regard to the EOM-IP/EA/DIP family of methods, orbital-relaxation effects are found to be more important than for particle-conserving EOM-EE/SF. Consequently, error bars for EOM-IP/EA-CCSD are larger than those of EOM-EE-CCSD; therefore, the inclusion of higher excitations (e.g.,  $3b2p$  for EOM-IP) seems to be necessary (94, 95). This is further exacerbated in EOM-DIP, in which the doubly attached reference often does not correspond to a physically bound state.

We can alleviate many of these problems (e.g., doubly excited states, spin contamination, and orbital relaxation) by including triples (or even higher excitations), at the price of the increased computational cost (e.g., full triples scale as  $N^8$ ). Alternatively, more practical solutions to many of these problems can be found in other regions of Fock space. Sometimes, a combination of several CC/EOM-CC schemes yields excellent results [see, for example, suggested Fock-space detours for calculating EAs in challenging open-shell systems (57) or diradical and triradical stabilization energies (75)].

## 6. CONCLUSIONS AND OUTLOOK: 53 MORE THINGS TO DO WITH EOM

As illustrated by the examples above, the single-reference EOM approach can describe many multiconfigurational wave functions by exploiting the advantages of the Fock space formalism, that is, by conceptual separation of the target and reference states. A journey in Fock space begins by identifying a reference from which the leading

configurations of the target states of interest can be described by the same-level excitations—preferably, but not necessarily, by the low-level ones. Established EOM-CC methods—EOM-EE/SF/IP/EA/DIP—enable access to many important types of open-shell wave functions (e.g., singly excited states, JT and pseudo-JT systems, radicals, diradicals, triradicals, and charge-transfer systems).

Of course, EOM does not offer a general solution to any imaginable open-shell situation. For example, multiple bond breaking and more extensive degeneracies in transition metals warrant explorations of other sectors of Fock space (e.g., double SF and SF-DEA), and I envision many successful ventures of this type in the future. However, some cases might remain accessible only through genuine MR approaches.

The EOM models are size consistent, and we can systematically improve their accuracy by including higher excitations explicitly or perturbatively. Elegant single-reference formalism facilitates implementation of analytic gradients, second derivatives, and property calculations (9, 13, 96–101). Moreover, the EOM methods are multistate schemes—several target states are obtained in a single diagonalization step. This results in an improved accuracy owing to built-in error cancellation and greatly simplifies the calculation of coupling matrix elements between states, such as nonadiabatic or spin-orbit couplings, or transition properties (e.g., Dyson orbitals for excited-state ionization) (102–104). The multistate nature of EOM along with the linear parameterization and simultaneous inclusion of dynamical and nondynamical correlation make EOM attractive for treating dense manifolds of states, conical intersections, and JT and pseudo-JT systems (18, 53), even though the theory's non-Hermitian properties pose certain challenges for the intersections between states of the same symmetry (59, 60).

Despite the impressive progress in EOM developments, more remains to be done, both technically and conceptually [e.g., second derivatives for EOM-SF, nonadiabatic couplings (105), and higher-order properties]. Other pressing issues include improving the accuracy in the computationally feasible scheme, for example, through perturbative rather than explicit inclusion of triple excitations (106–113), or the methods-of-moments approach (114, 115). Using active-space triples (39, 116–119) and/or energy-additivity schemes offers a solution. The similarity-transformed EOM-CC approach is also promising (120, 121). Spin adaptation of open-shell-based EOM-CC is another important issue, especially for the extension of EOM to higher-multiplicity references. It is discussed in detail in Reference 18.

Last, but not least, algorithmic improvements such as resolution-of-identity implementations (122–124), reduced-scaling algorithms (125, 126), and parallelization will address the scaling problem and extend EOM to larger systems.

I hope this review encourages the community to more aggressively exploit the advantages of EOM-CC. Indeed, the methods are well documented, and efficient EOM-CC codes are now available in many electronic-structure packages [e.g., Q-Chem (127), ACES II (128), MOLPRO (129), PSI3 (130), GAMESS (131), and DALTON (132)]. Rich and fascinating, the electronic structure of open-shell and EE species deserves to be explored using the best computational tools. The conceptual simplicity of EOM-CC, the robustness of single-reference implementation, and the bulk of applications demonstrating the capabilities of EOM allow even nonexperts to

see the marvels of the open-shell universe on their own, without the close involvement of electronic-structure specialists. Happy hitchhiking!

## DISCLOSURE STATEMENT

The author is not aware of any biases that might be perceived as affecting the objectivity of this review.

## ACKNOWLEDGMENTS

This work was conducted in the framework of the *IOpenShell* Center for Computational Studies of Electronic Structure and Spectroscopy of Open-Shell and Electronically Excited Species supported by the National Science Foundation through the CRIF:CRF CHE-0625419 + 0624602 + 0625237 grant. The results from our group discussed in this review were obtained with support from the National Science Foundation and the Department of Energy.

## LITERATURE CITED

1. Helgaker T, Jørgensen P, Olsen J. 2000. *Molecular Electronic Structure Theory*. New York: Wiley & Sons
2. Cramer CJ. 2002. *Essentials of Computational Chemistry: Theories and Models*. New York: Wiley & Sons
3. Hirao K, ed. 1999. *Recent Advances in Multi-Reference Methods*. Singapore: World Sci.
4. Roos BO, Taylor PR, Siegbahn PEM. 1980. A complete active space SCF method (CASSCF) using a density matrix formulated super-CI approach. *Chem. Phys.* 48:157–73
5. Ruedenberg K, Schmidt MW, Gilbert MM, Elbert ST. 1982. Are atoms intrinsic to molecular wavefunction? I. The FORS model. *Chem. Phys.* 71:41–49
6. Rowe DJ. 1968. Equations-of-motion method and the extended shell model. *Rev. Mod. Phys.* 40:153–66
7. Emrich K. 1981. An extension of the coupled-cluster formalism to excited states (I). *Nucl. Phys. A* 351:379–96
8. Geertsen J, Rittby M, Bartlett RJ. 1989. The equation-of-motion coupled-cluster method: excitation energies of Be and CO. *Chem. Phys. Lett.* 164:57–62
9. Stanton JF, Bartlett RJ. 1993. The equation of motion coupled-cluster method: a systematic biorthogonal approach to molecular excitation energies, transition probabilities, and excited state properties. *J. Chem. Phys.* 98:7029–39
10. Levchenko SV, Krylov AI. 2004. Equation-of-motion spin-flip coupled-cluster model with single and double substitutions: theory and application to cyclobutadiene. *J. Chem. Phys.* 120:175–85
11. Sinha D, Mukhopadhyay D, Mukherjee D. 1986. A note on the direct calculation of excitation energies by quasi-degenerate MBPT and coupled-cluster theory. *Chem. Phys. Lett.* 129:369–74

12. Pal S, Rittby M, Bartlett RJ, Sinha D, Mukherjee D. 1987. Multireference coupled-cluster methods using an incomplete model space: application to ionization potentials and excitation energies of formaldehyde. *Chem. Phys. Lett.* 137:273–78
13. Stanton JF, Gauss J. 1994. Analytic energy derivatives for ionized states described by the equation-of-motion coupled cluster method. *J. Chem. Phys.* 101:8938–44
14. Nooijen M, Bartlett RJ. 1995. Equation of motion coupled cluster method for electron attachment. *J. Chem. Phys.* 102:3629–47
15. **Mukherjee D, Pal S. 1989. Use of cluster expansion methods in the open-shell correlation problem. *Adv. Q. Chem.* 20:291–373**
16. Bartlett RJ, Stanton JF. 1994. Applications of post-Hartree-Fock methods: a tutorial. *Rev. Comp. Chem.* 5:65–169
17. **Bartlett RJ. 2002. To multireference or not to multireference: That is the question? *Int. J. Mol. Sci.* 3:579–603**
18. **Stanton JF, Gauss J. 2003. A discussion on some problems associated with the quantum mechanical treatment of open-shell molecules. *Adv. Chem. Phys.* 125:101–46**
19. Krylov AI. 2006. The spin-flip equation-of-motion coupled-cluster electronic structure method for a description of excited states, bond breaking, diradicals, and triradicals. *Acc. Chem. Res.* 39:83–91
20. Christiansen O. 2006. Coupled cluster theory with emphasis on selected new developments. *Theor. Chim. Acta* 116:106–23
21. Monkhorst HJ. 1977. Calculation of properties with the coupled-cluster method. *Int. J. Quant. Chem. Symp.* 11:421–32
22. Sekino H, Bartlett RJ. 1984. A linear response, coupled-cluster theory for excitation energy. *Int. J. Quant. Chem. Symp.* 18:255–65
23. Koch H, Jensen HJAa, Jørgensen P, Helgaker T. 1990. Excitation energies from the coupled clusters singles and doubles linear response functions (CCSDLR): applications to Be, CH<sup>+</sup>, CO, and H<sub>2</sub>O. *J. Chem. Phys.* 93:3345–50
24. Head-Gordon M, Lee TJ. 1997. Single reference coupled cluster and perturbation theories of electronic excitation energies. In *Modern Ideas in Coupled Cluster Theory*, ed. RJ Bartlett, pp. 221–53. Singapore: World Sci.
25. Nakatsuji H, Hirao K. 1978. Cluster expansion of the wavefunction: symmetry-adapted-cluster expansion, its variational determination, and extension of open-shell orbital theory. *J. Chem. Phys.* 68:2053–65
26. Nakatsuji H. 1991. Description of two- and many-electron processes by the SAC-CI method. *Chem. Phys. Lett.* 177:331–37
27. Jeziorski B, Monkhorst HJ. 1981. Coupled-cluster method for multideterminantal reference states. *Phys. Rev. A* 24:1668–81
28. Jeziorski B, Paldus J. 1989. Valence-universal exponential ansatz and the cluster structure of multireference configuration interaction wave function. *J. Chem. Phys.* 90:2714–31
29. **Evangelista FA, Allen WD, Schaefer HF. 2006. High-order excitations in state-universal and state-specific multireference coupled cluster theories: model systems. *J. Chem. Phys.* 125:154113**

---

15. Reviews different MR-CC approaches including Fock-space methods and EOM.

---

17. Discusses a relation between MR-CC, Fock space, and EOM methods.

---

18. Discusses in detail vibronic interactions and spin adaptation of EOM-CC.

---

---

29. Provides an overview of different MR-CC approaches and gives numerical examples.

---

30. Olsen J. 2000. The initial implementation and applications of a general active space coupled cluster method. *J. Chem. Phys.* 113:7140–48
31. Meissner L, Bartlett RJ. 1991. Transformation of the Hamiltonian in excitation energy calculations: comparison between Fock-space multireference coupled-cluster and equation-of-motion coupled-cluster methods. *J. Chem. Phys.* 94:6670–76
32. Nooijen M, Shamasundar KR, Mukherjee D. 2005. Reflections on size extensivity, size consistency, and generalized extensivity in many-body theory. *Mol. Phys.* 103:2277–98
33. Stanton JF. 1994. Separability properties of reduced and effective density matrices in the equation-of-motion coupled cluster method. *J. Chem. Phys.* 101:8928–37
34. Koch H, Kobayashi R, de Merás AS, Jørgensen P. 1994. Calculation of size-extensive transition moments from coupled cluster singles and doubles linear response function. *J. Chem. Phys.* 100:4393–400
35. Cizek J. 1966. On the correlation problem in atomic and molecular systems: calculation of wavefunction components in Ursell-type expansion using quantum-field theoretical methods. *J. Chem. Phys.* 45:4256–66
36. Purvis GD, Bartlett RJ. 1982. A full coupled-cluster singles and doubles model: the inclusion of disconnected triples. *J. Chem. Phys.* 76:1910–18
37. Kucharski SA, Wloch M, Musial M, Bartlett RJ. 2001. Coupled-cluster theory for excited electronic states: the full equation-of-motion coupled-cluster single, double, and triple excitation method. *J. Chem. Phys.* 115:8263–66
38. Hirata S, Nooijen M, Bartlett RJ. 2000. High-order determinantal equation-of-motion coupled-cluster calculations for electronic excited states. *Chem. Phys. Lett.* 326:255–62
39. Slipchenko LV, Krylov AI. 2005. Spin-conserving and spin-flipping equation-of-motion coupled-cluster method with triple excitations. *J. Chem. Phys.* 123:84107
40. Wladyslawski M, Nooijen M. 2002. The photoelectron spectrum of the NO<sub>3</sub> radical revisited: a theoretical investigation of potential energy surfaces and conical intersections. *ACS Symp. Ser.* 828:65–92
41. Sattelmeyer KW, Schaefer HF, Stanton JF. 2003. Use of 2h and 3h-p like coupled-cluster Tamm-Dancoff approaches for the equilibrium properties of ozone. *Chem. Phys. Lett.* 378:42–46
42. Krylov AI. 2001. Size-consistent wave functions for bond-breaking: the equation-of-motion spin-flip model. *Chem. Phys. Lett.* 338:375–84
43. Larsen H, Hald K, Olsen J, Jørgensen P. 2001. Triplet excitation energies in full configuration interaction and coupled-cluster theory. *J. Chem. Phys.* 115:3015–20
44. Fedorov I, Koziol L, Li G, Parr JA, Krylov AI, Reisler H. 2007. Theoretical and experimental investigations of electronic Rydberg states of diazomethane: assignments and state interactions. *J. Phys. Chem. A* 111:4557–66
45. Levchenko SV, Krylov AI. 2001. Electronic structure of halogen-substituted methyl radicals: excited states of CH<sub>2</sub>Cl and CH<sub>2</sub>F. *J. Chem. Phys.* 115:7485–94



46. Levchenko SV, Demyanenko AV, Dribinski V, Potter AB, Krylov AI, Reisler H. 2003. Rydberg-valence interactions in  $\text{CH}_2\text{Cl} \rightarrow \text{CH}_2 + \text{Cl}$  photodissociation: dependence of absorption probability on ground state vibrational excitation. *J. Chem. Phys.* 118:9233–40
  47. Gessner O, Lee AMD, Shaffer JP, Reisler H, Levchenko S, et al. 2006. Femtosecond multidimensional imaging of a molecular dissociation. *Science* 311:219–22
  48. Levchenko S, Reisler H, Krylov A, Gessner O, Stolow A, et al. 2006. Photodissociation dynamics of the NO dimer. I. Theoretical overview of the UV singlet excited states. *J. Chem. Phys.* 125:084301
  49. Koziol L, Levchenko SV, Krylov AI. 2006. Beyond vinyl: electronic structure of unsaturated propen-1-yl, propen-2-yl, 1-buten-2-yl, and trans-2-buten-2-yl hydrocarbon radicals. *J. Phys. Chem. A* 110:2746–58
  50. Mozhayskiy VA, Babikov D, Krylov AI. 2006. Conical and glancing Jahn-Teller intersections in the cyclic trinitrogen cation. *J. Chem. Phys.* 124:224309
  51. Babikov D, Mozhayskiy VA, Krylov AI. 2006. Photoelectron spectrum of elusive cyclic  $\text{N}_3$  and characterization of potential energy surface and vibrational states of the ion. *J. Chem. Phys.* 125:084306
  52. Dillon JJ, Yarkony DR. 2007. Seams near seams: the Jahn-Teller effect in the  $^1E'$  state of  $\text{N}_3^+$ . *J. Chem. Phys.* 126:124113
  53. Stanton JF. 2001. Coupled-cluster theory, pseudo-Jahn-Teller effects and conical intersections. *J. Chem. Phys.* 115:10382–93
  54. Stanton JF, Sattelmeyer KW, Gauss J, Allan M, Skalicky T, Bally T. 2001. On the photoelectron spectrum of p-benzoquinone. *J. Chem. Phys.* 115:1–4
  55. Ichino T, Gianola AJ, Lineberger WC, Stanton JF. 2006. Nonadiabatic effects in the photoelectron spectrum of the pyrazolide- $\text{d}_3$  anion: three-state interactions in the pyrazolyl- $\text{d}_3$  radical. *J. Chem. Phys.* 125:084312
  56. Vanovschi V, Krylov AI, Wenthold PG. 2007. Structure, vibrational frequencies, ionization energies, and photoelectron spectrum of the para-benzyne radical anion. *Theor. Chim. Acta*. In press
  57. Slipchenko LV, Krylov AI. 2006. **Efficient strategies for accurate calculations of electronic excitation and ionization energies: theory and application to the dehydro-meta-xylylene anion.** *J. Phys. Chem. A* 110:291–98
  58. Stanton JF. 2007. On the vibronic level structure in the  $\text{NO}_3$  radical. I. The ground electronic state. *J. Chem. Phys.* 126:134309
  59. Köhn A, Tajti A. 2007. **Can coupled-cluster theory treat conical intersections?** *J. Chem. Phys.* 127:044105
  60. Hättig C. 2005. Structure optimizations for excited states with correlated second-order methods: CC2 and ADC(2). *Adv. Quant. Chem.* 50:37–60
  61. Szalay PG, Gauss J. 2000. Spin-restricted open-shell coupled-cluster theory for excited states. *J. Chem. Phys.* 112:4027–36
  62. Maurice D, Head-Gordon M. 1995. Configuration interaction with single substitutions for excited states of open-shell molecules. *Int. J. Quant. Chem. Symp.* 29:361–70
- 
57. Calculates the EA of DMX by combining CCSD(T) and EOM-CC methods using computational schemes in the spirit of isodesmic reactions.
- 
59. Formal analysis and numeric examples demonstrating how the non-Hermitian nature of EOM affects the topology of conical intersections.
-

---

75. Develops and applies computational schemes for calculating accurate thermochemical values for the reactions involving diradicals and triradicals to characterize partial bonds between radical centers.

---

63. Krylov AI, Sherrill CD. 2002. Perturbative corrections to the equation-of-motion spin-flip SCF model: application to bond-breaking and equilibrium properties of diradicals. *J. Chem. Phys.* 116:3194–203
64. Krylov AI. 2001. Spin-flip configuration interaction: an electronic structure model that is both variational and size consistent. *Chem. Phys. Lett.* 350:522–30
65. Sears JS, Sherrill CD, Krylov AI. 2003. A spin-complete version of the spin-flip approach to bond breaking: What is the impact of obtaining spin eigenfunctions? *J. Chem. Phys.* 118:9084–94
66. Shao Y, Head-Gordon M, Krylov AI. 2003. The spin-flip approach within time-dependent density functional theory: theory and applications to diradicals. *J. Chem. Phys.* 118:4807–18
67. Slipchenko LV, Krylov AI. 2002. Singlet-triplet gaps in diradicals by the spin-flip approach: a benchmark study. *J. Chem. Phys.* 117:4694–708
68. Golubeva A, Nemukhin AV, Harding L, Klippenstein SJ, Krylov AI. 2007. Performance of spin-flip and multireference methods for bond-breaking in hydrocarbons: a benchmark study. *J. Phys. Chem. A*. In press
69. Slipchenko LV, Krylov AI. 2003. Electronic structure of the trimethylenemethane diradical in its ground and electronically excited states: bonding, equilibrium structures and vibrational frequencies. *J. Chem. Phys.* 118:6874–83
70. Wang T, Krylov AI. 2005. The effect of substituents on singlet-triplet energy separations in meta-xylylene diradicals: qualitative insights from quantitative studies. *J. Chem. Phys.* 123:104304
71. Krylov AI. 2005. Triradicals. *J. Phys. Chem. A* 109:10638–45
72. Slipchenko LV, Krylov AI. 2003. Electronic structure of the 1,3,5-tridehydrobenzene triradical in its ground and excited states. *J. Chem. Phys.* 118:9614–22
73. Slipchenko LV, Munsch TE, Wenthold PG, Krylov AI. 2004. 5-dehydro-1,3-quinodimethane: a hydrocarbon with an open-shell doublet ground state. *Angew. Chem. Int. Ed. Engl.* 43:742–45
74. Munsch TE, Slipchenko LV, Krylov AI, Wenthold PG. 2004. Reactivity and structure of the 5-dehydro-m-xylylene anion. *J. Org. Chem.* 69:5735–41
75. **Cristian AMC, Shao Y, Krylov AI. 2004. Bonding patterns in benzene triradicals from structural, spectroscopic, and thermochemical perspectives. *J. Phys. Chem. A* 108:6581–88**
76. Wang T, Krylov AI. 2006. Electronic structure of the two dehydro-meta-xylylene triradicals and their derivatives. *Chem. Phys. Lett.* 426:196–200
77. Koziol L, Winkler M, Houk KN, Venkataramani S, Sander W, Krylov AI. 2007. The 1,2,3-tridehydrobenzene triradical:  $^2B$  or not  $^2B$ ? The answer is  $^2A$ ! *J. Phys. Chem. A* 111:5071–80
78. Saeh JC, Stanton JF. 1999. Application of an equation-of-motion coupled cluster method including higher-order corrections to potential energy surfaces of radicals. *J. Chem. Phys.* 111:8275–85
79. Yang CH, Hsu CP. 2006. The dynamical correlation in spacer-mediated electron transfer couplings. *J. Chem. Phys.* 124:244507

80. Pieniazek PA, Arnstein SA, Bradforth SE, Krylov AI, Sherrill CD. 2007. Benchmark full configuration interaction and EOM-IP-CCSD results for prototypical charge transfer systems: noncovalent ionized dimers. *J. Chem. Phys.* 127:164110
81. Pieniazek PA, Krylov AI, Bradforth SE. 2007. Electronic structure of the benzene dimer cation. *J. Chem. Phys.* 127:044317
82. Nooijen M. 2002. State selective equation-of-motion coupled cluster theory: some preliminary results. *Int. J. Mol. Sci.* 3:656–75
83. McWeeny R. 1992. *Methods of Molecular Quantum Mechanics*. New York: Academic. 2nd ed.
84. Epstein ST. 1974. *The Variation Method in Quantum Chemistry*. New York: Academic
85. Löwdin P-O. 1982. On operators, superoperators, Hamiltonians and Liouvillians. *Int. J. Quant. Chem. Symp.* 16:485–560
86. Löwdin P-O. 1985. Some aspects on the Hamiltonian and Liouvillian formalism, the special propagator methods, and the equation of motion approach. *Adv. Q. Chem.* 17:285–334
87. McCurdy CW, Rescigno TN, Yeager DL, McKoy V. 1977. The equations of motion method: an approach to dynamical properties of atoms and molecules. In *Modern Theoretical Chemistry*, Vol. 3, pp. 339–86. New York: Plenum
88. Comeau DC, Bartlett RJ. 1993. The equation-of-motion coupled-cluster method: applications to open- and closed-shell reference states. *Chem. Phys. Lett.* 207:414–23
89. Szekeres Z, Szabados Á, Kállay M, Surján PR. 2001. On the “killer condition” in the equation-of-motion method: ionization potentials from multi-reference wave functions. *Phys. Chem. Chem. Phys.* 3:696–701
90. Purvis GD III, Sekino H, Bartlett RJ. 1988. Multiplicity of many-body wavefunctions using unrestricted Hartree-Fock reference functions. *Collect. Czech. Chem. Commun.* 53:2203–13
91. Stanton JF. 1994. On the extent of spin contamination in open-shell coupled-cluster wave functions. *J. Chem. Phys.* 101:371–74
92. Sherrill CD, Krylov AI, Byrd EFC, Head-Gordon M. 1998. Energies and analytic gradients for a coupled-cluster doubles model using variational Brueckner orbitals: application to symmetry breaking in  $O_4^+$ . *J. Chem. Phys.* 109:4171–81
93. Krylov AI, Sherrill CD, Head-Gordon M. 2000. Excited states theory for optimized orbitals and valence optimized orbitals coupled-cluster doubles models. *J. Chem. Phys.* 113:6509–27
94. Hirata S, Nooijen M, Bartlett RJ. 2000. High-order determinantal equation-of-motion coupled-cluster calculations for ionized and electron-attached states. *Chem. Phys. Lett.* 328:459–68
95. Kamya M, Hirata S. 2006. Higher-order equation-of-motion coupled-cluster methods for ionization processes. *J. Chem. Phys.* 125:074111
96. Stanton JF. 1993. Many-body methods for excited state potential energy surfaces. I. General theory of energy gradients for the equation-of-motion coupled-cluster method. *J. Chem. Phys.* 99:8840–47

97. Stanton JF, Gauss J. 1995. Many-body methods for excited state potential energy surfaces. II. Analytic second derivatives for excited state energies in the equation-of-motion coupled-cluster method. *J. Chem. Phys.* 103:88931
98. Levchenko SV, Wang T, Krylov AI. 2005. Analytic gradients for the spin-conserving and spin-flipping equation-of-motion coupled-cluster models with single and double substitutions. *J. Chem. Phys.* 122:224106
99. Gauss J, Stanton JF. 2002. Electron-correlated approaches for the calculation of NMR chemical shifts. *Adv. Chem. Phys.* 123:355-422
100. Crawford TD. 2006. Ab initio calculation of molecular chiroptical properties. *Theor. Chim. Acta* 115:227-45
101. Hättig C, Christiansen O, Jørgensen P. 1998. Multiphoton transition moments and absorption cross sections in coupled cluster response theory employing variational transition moment functionals. *J. Chem. Phys.* 108:8331-54
102. Epifanovsky E, Krylov AI. 2007. Direct location of the minimum point on intersection seams of potential energy surfaces with equation-of-motion coupled-cluster methods. *Mol. Phys.* In press
103. Christiansen O, Gauss J, Schimmelpfennig B. 2000. Spin-orbit coupling constants from coupled-cluster response theory. *Phys. Chem. Chem. Phys.* 2:965-71
104. Oana M, Krylov AI. 2007. Dyson orbitals for ionization from the ground and electronically excited states within equation-of-motion formalism: theory, implementation and examples. *J. Chem. Phys.* In press
105. Stanton JF, Gauss J. 2007. A quasidiabatic approach in equation-of-motion coupled cluster theory: perspective, derivations and preliminary applications. Private communication
106. Noga J, Bartlett RJ, Urban M. 1987. Towards a full CCSDT model for electron correlation: CCSDT-n models. *Chem. Phys. Lett.* 134:126-32
107. Watts JD, Bartlett RJ. 1995. Economical triple excitation equation-of-motion coupled-cluster methods for excitation energies. *Chem. Phys. Lett.* 233:81-87
108. Watts JD, Bartlett RJ. 1996. Iterative and noniterative triple excitation corrections in coupled-cluster methods for excited electronic states: the EOM-CCSDT-3 and EOM-CCSD( $\bar{T}$ ) methods. *Chem. Phys. Lett.* 258:581-88
109. Koch H, Christiansen O, Jørgensen P, de Meras AMS, Helgaker T. 1997. The CC3 model: an iterative coupled cluster approach including connected triples. *J. Chem. Phys.* 106:1808-18
110. Koch H, Christiansen O, Jørgensen P, Olsen J. 1995. Excitation energies of BH, CH<sub>2</sub>, and Ne in full configuration interaction and the hierarchy CCS, CC2, CCSD, and CC3 of coupled cluster models. *Chem. Phys. Lett.* 244:75-82
111. Christiansen O, Koch H, Jørgensen P. 1995. Response functions in the CC3 iterative triple excitation model. *J. Chem. Phys.* 103:7429-41
112. Smith CE, King RA, Crawford TD. 2005. Coupled cluster methods including triple excitations for excited states of radicals. *J. Chem. Phys.* 122:054110
113. Sattelmeyer KW, Stanton JF, Olsen J, Gauss J. 2001. A comparison of excited state properties for iterative approximate triples linear response coupled cluster methods. *Chem. Phys. Lett.* 347:499-504

114. Piecuch P, Wloch M. 2005. Renormalized coupled-cluster methods exploiting left eigenstates of the similarity transformed Hamiltonian. *J. Chem. Phys.* 123:224105
115. Piecuch P, Kowalski K, Pimienta ISO, McGuire MJ. 2002. Recent advances in electronic structure theory: method of moments of coupled-cluster equations and renormalized coupled-cluster approaches. *Int. Rev. Phys. Chem.* 21:527–655
116. Kowalski K, Piecuch P. 2000. The active-space equation-of-motion coupled-cluster methods for excited electronic states: the EOMCCSDt approach. *J. Chem. Phys.* 113:8490–502
117. Kowalski K, Piecuch P. 2001. The active-space equation-of-motion coupled-cluster methods for excited electronic states: full EOMCCSDt. *J. Chem. Phys.* 115:643–51
118. Gour J, Piecuch P. 2006. Efficient formulation and computer implementation of the active-space electron-attached and ionized equation-of-motion coupled-cluster methods. *J. Chem. Phys.* 125:234107
119. Fan PD, Kamiya M, Hirata S. 2007. Active-space equation-of-motion coupled-cluster methods through quadruples for excited, ionized, and electron-attached states. *J. Chem. Theory Comput.* 3:1036–46
120. Nooijen M, Bartlett RJ. 1997. Similarity transformed equation-of-motion coupled-cluster study of ionized, electron attached, and excited states of free base porphyrin. *J. Chem. Phys.* 106:6449–55
121. Nooijen M, Bartlett RJ. 1997. Similarity transformed equation-of-motion coupled-cluster theory: details, examples, and comparisons. *J. Chem. Phys.* 107:6812–30
122. Hättig C, Hald K. 2002. Implementation of RI-CC2 triplet excitation energies with an application to *trans*-azobenzene. *Phys. Chem. Chem. Phys.* 4:2111–18
123. Köhn A, Hättig C. 2003. Analytic gradients for excited states in the coupled-cluster model CC2 employing the resolution-of-the-identity approximation. *J. Chem. Phys.* 119:5021–36
124. Rhee YM, Head-Gordon M. 2007. Scaled second-order perturbation corrections to configuration interaction singles: efficient and reliable excitation energy methods. *J. Phys. Chem. A* 111:5314–26
125. Korona T, Werner HJ. 2003. Local treatment of electron excitations in the EOM-CCSD method. *J. Chem. Phys.* 118:3006–19
126. Kats D, Korona T, Schütz M. 2006. Local CC2 electronic excitation energies for large molecules with density fitting. *J. Chem. Phys.* 125:104106
127. Shao Y, Molnar LF, Jung Y, Kussmann J, Ochsenfeld C, et al. 2006. Advances in methods and algorithms in a modern quantum chemistry program package. *Phys. Chem. Chem. Phys.* 8:3172–91
128. Stanton JF, Gauss J, Watts JD, Lauderdale WJ, Bartlett RJ. 1993. ACES II software.
129. Werner H-J, Knowles PJ, Lindh R, Manby FR, Schütz M, et al. 2007. Molpro version 2006.1. <http://www.molpro.net>

130. Crawford TD, Sherrill CD, Valeev EF, Fermann JT, King RA, et al. 2007. PSI3: an open-source ab initio electronic structure package. *J. Comput. Chem.* 28:1610–16
131. Schmidt MW, Baldrige KK, Boatz JA, Elbert ST, Gordon MS, et al. 1993. General atomic and molecular electronic structure system. *J. Comput. Chem.* 14:1347–63
132. DALTON. 2005. Release 2.0. <http://www.kjemi.uio.no/software/dalton/dalton.html>



# Contents

A Fortunate Life in Physical Chemistry <i>Stuart A. Rice</i> .....	1
Chemistry and Photochemistry of Mineral Dust Aerosol <i>David M. Cwiertny, Mark A. Young, and Vicki H. Grassian</i> .....	27
Femtobiology <i>Villy Sundström</i> .....	53
Structures, Kinetics, Thermodynamics, and Biological Functions of RNA Hairpins <i>Philip C. Bevilacqua and Joshua M. Blose</i> .....	79
Understanding Protein Evolution: From Protein Physics to Darwinian Selection <i>Konstantin B. Zeldovich and Eugene I. Shakhnovich</i> .....	105
Quasicrystal Surfaces <i>Patricia A. Thiel</i> .....	129
Molecular Ordering and Phase Behavior of Surfactants at Water-Oil Interfaces as Probed by X-Ray Surface Scattering <i>Mark L. Schlossman and Aleksey M. Tikhonov</i> .....	153
Extraordinary Transmission of Metal Films with Arrays of Subwavelength Holes <i>James V. Coe, Joseph M. Heer, Shannon Teeters-Kennedy, Hong Tian, and Kenneth R. Rodriguez</i> .....	179
The Ultrafast Dynamics of Photodetachment <i>Xiyi Chen and Stephen E. Bradforth</i> .....	203
Energy Flow in Proteins <i>David M. Leitner</i> .....	233
Advances in Correlated Electronic Structure Methods for Solids, Surfaces, and Nanostructures <i>Patrick Huang and Emily A. Carter</i> .....	261
Two-Dimensional Infrared Spectroscopy of Photoswitchable Peptides <i>Peter Hamm, Jan Helbing, and Jens Bredenbeck</i> .....	291

Wave-Packet Interferometry and Molecular State Reconstruction: Spectroscopic Adventures on the Left-Hand Side of the Schrödinger Equation <i>Jeffrey A. Cina</i> .....	319
Ions at Aqueous Interfaces: From Water Surface to Hydrated Proteins <i>Pavel Jungwirth and Bernd Winter</i> .....	343
Nanografting for Surface Physical Chemistry <i>Maozi Liu, Nabil A. Amro, and Gang-yu Liu</i> .....	367
Extending X-Ray Crystallography to Allow the Imaging of Noncrystalline Materials, Cells, and Single Protein Complexes <i>Jianwei Miao, Tetsuya Ishikawa, Qun Shen, and Thomas Earnest</i> .....	387
Patterning Fluid and Elastomeric Surfaces Using Short-Wavelength UV Radiation and Photogenerated Reactive Oxygen Species <i>Babak Sanii and Atul N. Parikh</i> .....	411
Equation-of-Motion Coupled-Cluster Methods for Open-Shell and Electronically Excited Species: The Hitchhiker's Guide to Fock Space <i>Anna I. Krylov</i> .....	433
Attosecond Electron Dynamics <i>Matthias F. Kling and Marc J.J. Vrakking</i> .....	463
Functional Polymer Brushes in Aqueous Media from Self-Assembled and Surface-Initiated Polymers <i>Ryan Toomey and Matthew Tirrell</i> .....	493
Electronic Spectroscopy of Carbon Chains <i>Evan B. Jochowitz and John P. Maier</i> .....	519
Multiscale Simulation of Soft Matter: From Scale Bridging to Adaptive Resolution <i>Matej Praprotnik, Luigi Delle Site, and Kurt Kremer</i> .....	545
Free Energies of Chemical Reactions in Solution and in Enzymes with Ab Initio Quantum Mechanics/Molecular Mechanics Methods <i>Hao Hu and Weitao Yang</i> .....	573
Fluctuation Theorems <i>E.M. Sevick, R. Prabhakar, Stephen R. Williams, and Debra J. Searles</i> .....	603
Structure, Dynamics, and Assembly of Filamentous Bacteriophages by Nuclear Magnetic Resonance Spectroscopy <i>Stanley J. Opella, Ana Carolina Zeri, and Sang Ho Park</i> .....	635
Inside a Collapsing Bubble: Sonoluminescence and the Conditions During Cavitation <i>Kenneth S. Suslick and David J. Flannigan</i> .....	659



Elastic Modeling of Biomembranes and Lipid Bilayers <i>Frank L.H. Brown</i> .....	685
Water in Nonpolar Confinement: From Nanotubes to Proteins and Beyond <i>Jayendran C. Rasaiah, Shekhar Garde, and Gerhard Hummer</i> .....	713
High-Resolution Spectroscopic Studies and Theory of Parity Violation in Chiral Molecules <i>Martin Quack, Jürgen Stobner, and Martin Willeke</i> .....	741
Collapse Mechanisms of Langmuir Monolayers <i>Ka Yee C. Lee</i> .....	771

## Indexes

Cumulative Index of Contributing Authors, Volumes 55–59 .....	793
Cumulative Index of Chapter Titles, Volumes 55–59 .....	796

## Errata

An online log of corrections to *Annual Review of Physical Chemistry* articles may be found at <http://physchem.annualreviews.org/errata.shtml>